1-D Open-Channel Flow Simulation Using TVD-McCormack Scheme

By P. García-Navarro,[1] F. Alcrudo,[2] and J. M. Savirón[3]

Abstract: The addition of a dissipation step to the widely used McCormack numerical scheme is proposed for solving one-dimensional open-channel flow equations. The extra step is devised according to the theory of total variation diminishing (TVD) schemes that are capable of capturing sharp discontinuities without generating the spurious oscillations that more classical methods do. At the same time, the extra step does not introduce any additional difficulty for the treatment of the source terms of the equations. Results from several computations are presented and comparison with the analytical solution for some test problems is shown. The overall performance of the method can be considered very good, and it allows for accurate open-channel flow computations involving hydraulic jumps and bores.

Introduction

Determination of the flow variables for different situations of a considered hydraulic system is often needed for a useful evaluation of a waterway's performance. One adopted approach is to construct a physical model of the system in order to carry out tests that may lead to conclusions about the flow situations that are likely to occur and their consequences. An alternative engineering technique is the matematical modeling of the hydraulic situation under consideration (Cunge et al. 1980). Assuming that a given set of equations, under certain approximations, describes the flow behavior, the resolution of the equations will provide the practitioner with the needed information. Very frequently this latter approach can solve the problem at a lower cost than the former one.

In the case of open-channel flow hydraulics, it is now common practice to use mathematical models mainly based on the shallow-water or Saint Venant equations to numerically simulate steady as well as unsteady phenomena. Calculation of equilibrium profiles or flood routings becomes possible with the aid of these models. The nonlinearity of the governing equations may, however, render their resolution rather complicated in the sense that they can only be solved numerically, and gives rise to the possibility of the appearance of discontinuous solutions, which are the mathematical counterpart of phenomena such as hydraulic jumps and bores (Stoker 1957). Solutions of that kind usually appear when modeling steady flows in steeply sloping channels, rapidly varied steady and unsteady flows, or in dam collapse simulations. In all these cases the adopted numerical treatment is of paramount importance in what concerns the quality of the results, often with a shock-capturing method of second order of accuracy being required.

[1]Asst. Prof., Dept. de Ciencia y Tecnología de Materiales y Fluidos, Facultad de Ciencias (Físicas), Univ. de Zaragoza, 50009 Zaragoza, Spain.

[2]Postgrad. Student, Dept. de Ciencia y Tecnología de Materiales y Fluidos, Facultad de Ciencias (Físicas), Univ. de Zaragoza, 50009 Zaragoza, Spain.

[3]Prof., Dept. de Ciencia y Tecnología de Materiales y Fluidos, Facultad de Ciencias (Físicas), Univ. de Zaragoza, 50009 Zaragoza, Spain.

Note. Discussion open until March 1, 1993. To extend the closing date one month, a written request must be filed with the ASCE Manager of Journals. The manuscript for this paper was submitted for review and possible publication on June 10, 1991. This paper is part of the ***Journal of Hydraulic Engineering***, Vol. 118, No. 10, October, 1992. ©ASCE, ISSN 0733-9429/92/0010-1359/$1.00 + $.15 per page. Paper No. 2069.

It is well known that all these classical methods present oscillations around discontinuities, which degrade the accuracy of the numerical solution and are difficult to remove if a general method of resolution is sought.

During the last decade much effort has been devoted to the numerical solution of systems of conservation laws, mainly driven by the need for efficient Euler solvers in aerodynamics. This has led to a new class of methods that do not suffer from the known penalties of classical ones (Hirsch 1990; Roe 1989) and to a generation of techniques able to improve the performance of conservative second-order classical schemes. It is the main purpose of this paper to report on the implementation of this technique onto the expicit McCormack scheme and to report the results obtained for the simulation of several hydraulic phenomena with its aid.

Mathematical Model Describing 1-D Open Channel Flow

One-dimensional open-channel flow is usually described in terms of water depth and discharge, and the evolution of these quantitites is taken to be governed by the Saint Venant equations, which simply express the conservation of mass and momentum along the flow direction (Cunge et al. 1980). The hypotheses under which this description is meaningful can be summarized as follows.

1. Flow is one dimensional (1-D). In this sense, velocity distribution is taken to be uniform in every cross section.
2. Pressure distribution is hydrostatic.
3. Bottom slope is very small.
4. Variations of channel shape with distance are very smooth.
5. Friction at the bottom and walls of the channel is dominant over internal shear stresses, and these can thus be neglected. It is also supposed that the friction force can be approximated by the formulas used in steady uniform flow.

The more restrictive among these hypotheses will depend obviously on the actual hydraulic situation. It can be generally stated that natural river flows are the most difficult to be well represented by the model; artificial, man-made channels follow the foregoing hypotheses more closely.

Under these assumptions the equations that model 1-D open-channel flow (Saint Venant equations) can be written in conservative or divergent form as

$$\frac{\partial \mathbf{U}}{\partial t} + \frac{\partial \mathbf{F}}{\partial x} = \mathbf{G} \quad \ldots\ldots (1)$$

where

$$\mathbf{U} = \begin{pmatrix} A \\ Q \end{pmatrix} \quad \ldots\ldots (2a)$$

$$\mathbf{F} = \begin{pmatrix} Q \\ \dfrac{Q^2}{A} + gI_1 \end{pmatrix} \quad \ldots\ldots (2b)$$

$$\mathbf{G} = \begin{bmatrix} 0 \\ gI_2 + gA(S_0 - S_f) \end{bmatrix} \quad \ldots\ldots (2c)$$

$A[x, h(x, t)]$ = wetted cross-section area; h = water depth; $Q(x, t)$ = discharge; g = acceleration of gravity; and I_1 = hydrostatic pressure force term that can be written

$$I_1 = \int_0^{h(x,t)} [h - \eta]\sigma(x, \eta)\, d\eta \quad \ldots\ldots (3)$$

with σ

$$\sigma(x, \eta) = \frac{\partial A(x, \eta)}{\partial \eta} \quad \ldots\ldots (4)$$

This represents the channel width at the free surface for a water depth of η. The term I_2 appearing in the source term is defined as follows:

$$I_2 = \int_0^{h(x,t)} [h - \eta] \frac{\partial \sigma(x, \eta)}{\partial x}\, d\eta \quad \ldots\ldots (5)$$

Eq. (5) accounts for the forces exerted by the channel walls at contractions and expansions; S_0 and S_f = bottom and friction slopes, respectively, the latter one being approximated by any of the empirical laws available in the literature (French 1985). In the present work, Manning's formula is used.

Two sources of difficulty may arise when numerically integrating (1). One of them is related to the flux vector function **F**, which, being nonlinear, is responsible for the appearance of discontinuous solutions. The other stems from the presence of a source term.

It is interesting to write the Jacobian matrix of the flux

$$\mathbf{J} = \frac{\partial \mathbf{F}}{\partial \mathbf{U}} = \begin{bmatrix} 0 & 1 \\ gA/\sigma - Q^2/A^2 & 2Q/A \end{bmatrix} \quad \ldots\ldots (6)$$

which has as eigenvalues and eigenvectors

$$a^{1,2} = u \pm c \quad \ldots\ldots (7a)$$

$$\mathbf{e}^{1,2} = \begin{pmatrix} 1 \\ u \pm c \end{pmatrix} \quad \ldots\ldots (7b)$$

$$u = \frac{Q}{A} \quad \ldots\ldots (8a)$$

$$c = \sqrt{\frac{gA}{\sigma}} \quad \ldots\ldots (8b)$$

The eigenvalues of **J** are the characteristic speeds, and their signs provide information about the directions of propagation of perturbations in the flow. With the use of **J**, an equivalent but nonconservative form of (1) is

$$\frac{\partial \mathbf{U}}{\partial t} + \mathbf{J}\frac{\partial \mathbf{U}}{\partial x} = \mathbf{G} \quad \ldots\ldots (9)$$

When modeling flows capable of developing discontinuities, the conser-

vative form of the equations, (1), is to be preferred to (9) since it guarantees correct jump intensities and celerities (Lax and Wendroff 1960).

TVD-McCormack Scheme

To solve (1) by means of a numerical time-stepping procedure, the domain of integration is discretized as $x_j = j\Delta x$; $t^n = n\Delta t$, where Δt and Δx = uniform mesh spacings.

The presence of a source term together with the requirement of second-order accuracy in both space and time makes impossible the use of a one-step algorithm without a cumbersome treatment. Hence, the presented high-resolution scheme is based on McCormack's two-step procedure, which reads (McCormack 1971)

$$\mathbf{U}_j^p = \mathbf{U}_j^n - \lambda(\mathbf{F}_{j+1}^n - \mathbf{F}_j^n) + \Delta t \mathbf{G}_j^n \quad \ldots\ldots (10a)$$

$$\mathbf{U}_j^c = \mathbf{U}_j^n - \lambda(\mathbf{F}_j^p - \mathbf{F}_{j-1}^p) + \Delta t \mathbf{G}_j^p \quad \ldots\ldots (10b)$$

where superindexes p and c stand for predictor and corrector steps; $\lambda = \Delta t/\Delta x$; and $F_j = F(U_j)$.

The solution at the next time level becomes

$$\mathbf{U}_j^{n+1} = \frac{1}{2}(\mathbf{U}_j^p + \mathbf{U}_j^c) \quad \ldots\ldots (11)$$

A third step is proposed in this paper. It furnishes the scheme with total variation diminishing (TVD) dissipation capable of rendering the solution oscillation free while retaining second-order accuracy in space and time almost everywhere (except at extrema points) (Harten 1984; Yee 1989; Hirsch 1990). This is a very remarkable property indeed when dealing with supercritical and rapidly varied flows with hydraulic jumps and bores. To achieve this, (11) is replaced by

$$\mathbf{U}_j^{n+1} = \frac{1}{2}(\mathbf{U}_j^p + \mathbf{U}_j^c) + \lambda(\mathbf{D}_{j+1/2}^n - \mathbf{D}_{j-1/2}^n) \quad \ldots\ldots (12)$$

The form of the D term is

$$\mathbf{D}_{j+1/2}^n = \frac{1}{2}\sum_{k=1}^{2} \alpha_{j+1/2}^k \Psi(\bar{a}_{j+1/2}^k)(1 - \lambda|\bar{a}_{j+1/2}^k|)[1 - \phi(r_{j+1/2}^k)]\bar{\mathbf{e}}_{j+1/2}^k \quad \ldots (13)$$

where $\bar{a}_{j+1/2}^k$ = a discrete average characteristic speed of the states at j and $j + 1$, expressed as

$$\bar{a}_{j+1/2}^{1,2} = \bar{u}_{j+1/2} \pm \bar{c}_{j+1/2} \quad \ldots\ldots (14)$$

and $\bar{\mathbf{e}}_{j+1/2}^k$ = discrete eigenvectors of the associated approximate Jacobian

$$\bar{\mathbf{e}}_{j+1/2}^{1,2} = \begin{pmatrix} 1 \\ \bar{a}_{j+1/2}^{1,2} \end{pmatrix} \quad \ldots\ldots (15)$$

The quantities $\bar{u}_{j+1/2}$ and $\bar{c}_{j+1/2}$ = discrete approximations to the water velocity and speed of sound, defined by

$$\bar{u}_{j+1/2} = \frac{\dfrac{Q_{j+1}}{\sqrt{A_{j+1}}} + \dfrac{Q_j}{\sqrt{A_j}}}{\sqrt{A_{j+1}} + \sqrt{A_j}} \quad \ldots\ldots (16)$$

$$\bar{c}^2_{j+1/2} = g\frac{I_{1j+1} - I_{1j}}{A_{j+1} - A_j} \quad \ldots\ldots (17a)$$

$$\bar{c}^2_{j+1/2} = \left(\frac{c_{j+1} + c_j}{2}\right)^2 \quad \ldots\ldots (17b)$$

The alternative definition of $\bar{c}_{j+1/2}$ is stated to cope with situations in which the areas of two adjacent wetted cross sections are the same, or the variation of the wetted cross-section area along the channel does not have the same sign as that of the hydrostatic pressure distribution. The $\alpha^k_{j+1/2}(k = 1,2)$ represent the projections of the jump in the values of $\mathbf{U}$ between the state at j and at $j + 1$, onto the approximate eigenvectors $\bar{\mathbf{e}}^k_{j+1/2}$ (Roe 1981; Glaister 1988)

$$\alpha^{1,2}_{j+1/2} = \frac{\pm 1}{2\bar{c}_{j+1/2}}[(Q_{j+1} - Q_j) + (-\bar{u}_{j+1/2} \pm \bar{c}_{j+1/2})(A_{j+1/2} - A_j)] \quad \ldots (18)$$

The function Ψ is an entropy correction to $\bar{a}^k_{j+1/2}$, and, in its simplest expression, takes the form

$$\Psi(a) = |a| \quad \text{if } |a| \geq \delta \quad \ldots\ldots (19a)$$

$$\Psi(a) = \delta \quad \text{if } |a| < \delta \quad \ldots\ldots (19b)$$

where δ = a small positive number (between 0.1 and 0.3). This correction prevents the appearance of unphysical hydraulic jumps; i.e., those in which energy increases across the shock, which are admissible for the classical McCormack scheme (Yee 1989). Other forms of the entropy correction may be applied (Sweby 1982; Harten and Hyman 1983).

Finally, the factor φ in (13) is a limiter, responsible for obtaining non-oscillatory solutions despite the presence of strong gradients or shocks. It is a nonlinear function of the ratio

$$r^k_{j+1/2} = \frac{\alpha^k_{j+1/2-S}}{\alpha^k_{j+1/2}}; \qquad s = \text{sign}(a^k_{j+1/2}) \quad \ldots\ldots (20)$$

Several forms of the function φ can be found in the literature (Sweby 1984; Roe 1984; Hirsch 1990). Their effect is basically the same for all of them, and consists of adding sufficient artificial dissipation to the scheme when there is a discontinuity or a steep gradient in the solution so that it remains monotone, while adding very little or no dissipation in regions of smooth variation.

It should be stressed that, strictly speaking, the theory of high resolution TVD schemes has been rigorously developed only for homogeneous nonlinear scalar equations or for homogeneous linear systems. However, numerical evidence, mainly in the field of aerodynamics, shows accurate and monotone results also for nonlinear systems of equations. The present work evidences a very good performance of the method for the nonlinear open-channel flow equations with inclusions of the source terms.

The stability of the scheme described by (10 and 12) is difficult to analyze in the nonlinear case because the corrector step involves values calculated in the predictor step. However, in the linear equation case it can be shown that scheme of (10 and 12) is identical to Lax-Wendroff method plus the numerical dissipation given by (12). Thus, although not rigorously true,

results obtained for the TVD Lax-Wendroff scheme concerning stability and monotonicity will be taken as valid for the proposed scheme too.

TVD Lax-Wendroff scheme is easier to analyze because it is a single-step algorithm, but it presents the drawback that inclusion of source terms is not as straightforward as it is for a predictor-corrector method. The scheme's stability is guaranteed in both the linear and nonlinear homogeneous scalar equation as well as for the linear homogeneous system case by the TVD property (expressed here as being capable of producing monotone or non-oscillatory solutions), which is a stronger requirement than stability and that imposes a limit on the Courant-Friedrichs-Levy (CFL) number given by (Sweby 1984)

$$CFL_{max} = \frac{2}{2 + \varphi_{max}} \quad \text{(21)}$$

where φ_{max} = maximum value attainable by the limiting function, which varies between 1 and 2. Nevertheless, and despite the fact that the case dealt with here is a nonlinear inhomogeneous system, experience shows that monotone calculations can be performed up to CFL numbers close to 1, which is the stability limit for standard Lax-Wendroff or McCormack schemes.

Numerical instabilities can also arise from the presence of the source term (Gunaratnam and Perkins 1970; Huang and Song 1985). A way to relax the corresponding restrictions on the time step would be to treat the source term implicitly. This would not affect substantially the computational efficiency of the method, since the corresponding discrete implicit operator would be a diagonal matrix and thus straightforward to invert. If such a treatment is carried out, the time-step restriction due to the source term is strongly relaxed.

Numerical Results

In this section, the numerical results are exhibited that were obtained for several test problems used to validate the described algorithm.

All the examples consider either rectangular or trapezoidal channels and include some type of source term. In all of the examples, the treatment of the external as well as internal boundary conditions is based on the theory of the characteristics (García-Navarro and Savirón 1990), and the limiting function φ used is that proposed by Van Leer (Roe 1984; Sweby 1984). Comparisons with the exact solution, when available, and with the plain McCormack scheme are shown.

Flow over Ladder of Weirs

The first example is concerned with the computation of the discontinuous stationary flow in a 500 m long rectangular channel 6 m wide (b = 6 m) that contains three identical weirs of height (H_v) 0.25 m. The bottom slope S_0 = 0.008 and the roughness, n = 0.015 are included in the source terms of the equations. The initial conditions are $Q(x, 0)$ = 20 m^3/s; and $h(x, 0)$ = 2 m. For the flow over the internal weirs, the characteristics equations together with mass continuity and a rate flow relationship $Q = Q(h)$ to define the presence of the weir are used while the flow is subcritical. Once it becomes critical at the right side point of the weir, the critical depth at that point is kept fixed as the second boundary condition (instead of the backward characteristic). The numerical scheme locates the sharp discontinuities of the corresponding stationary solution, preventing the appearance

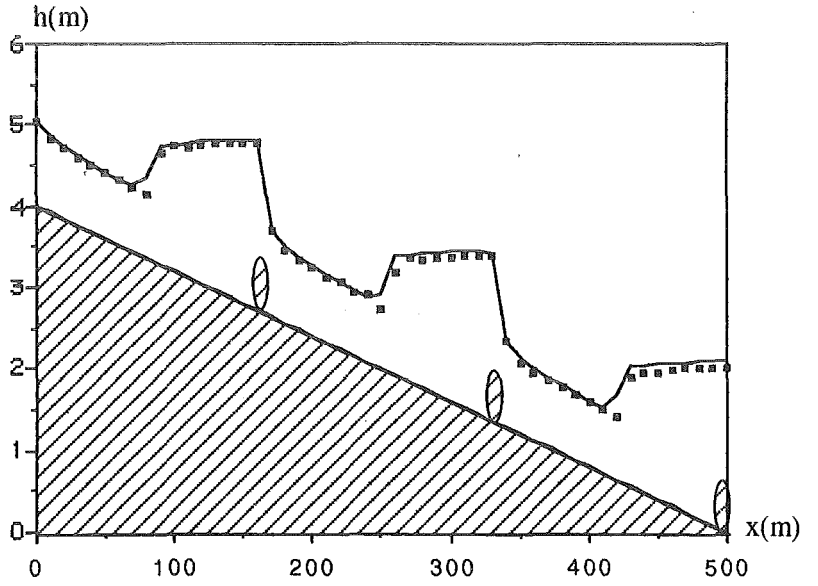

FIG. 1. Computation of Discontinuous Steady Flow over Ladder of Weirs with Bottom Slope and Friction on Rectangular Channel (—— = Computed with TVD McCormack scheme; ■ = Computed with Classical McCormack Scheme)

of oscillations around them. The results of the calculations made with the plain and the modified McCormack schemes on a $\Delta x = 10$ m grid with a CFL = 0.9 can be observed in Fig. 1. The classical method is still widely used in computational hydraulics for its simplicity and good performance in the presence of not very strong jumps. Small oscillations are nevertheless present around the discontinuities. The TVD McCormack scheme provides a more accurate steady state devoid of oscillations.

Flood Wave Propagation in Sloping Trapezoidal Channel

The same type of source terms appears in the second example corresponding to Figs. 2 and 3. It was run for a trapezoidal channel 6 m wide at the bottom, with a lateral wall slope (horizontal to vertical) of 0.25. Three regions can be labeled by their different bed slopes ($S_{01} = 0.002$; $S_{02} = 0.009$; $S_{03} = 0.001$). The friction coefficient and CFL number are the same as previously; 51 mesh points were used in the spatial discretization.

The initial conditions are given by a previously computed discontinuous steady profile corresponding to a discharge of $Q(x, 0) = 20$ m^3/s. A flood hydrograph [$Q = Q(t)$] is introduced at the upstream boundary by a sudden increase of the discharge to $Q = 50$ m^3/s, which persists for a time interval of 30 s. This means a supercritical advancing surge, and therefore requires two upstream boundary conditions. The second upstream boundary condition stems from the value of the water level that satisfies the mass and momentum conservation relationships across the shock (García-Navarro 1989). Then the discharge is linearly reduced to its initial value during another 30 s. Once the flow becomes subcritical there, use is made of the characteristics for the upstream boundary condition. The downstream boundary is determined by a stage-discharge rating curve on the weir type

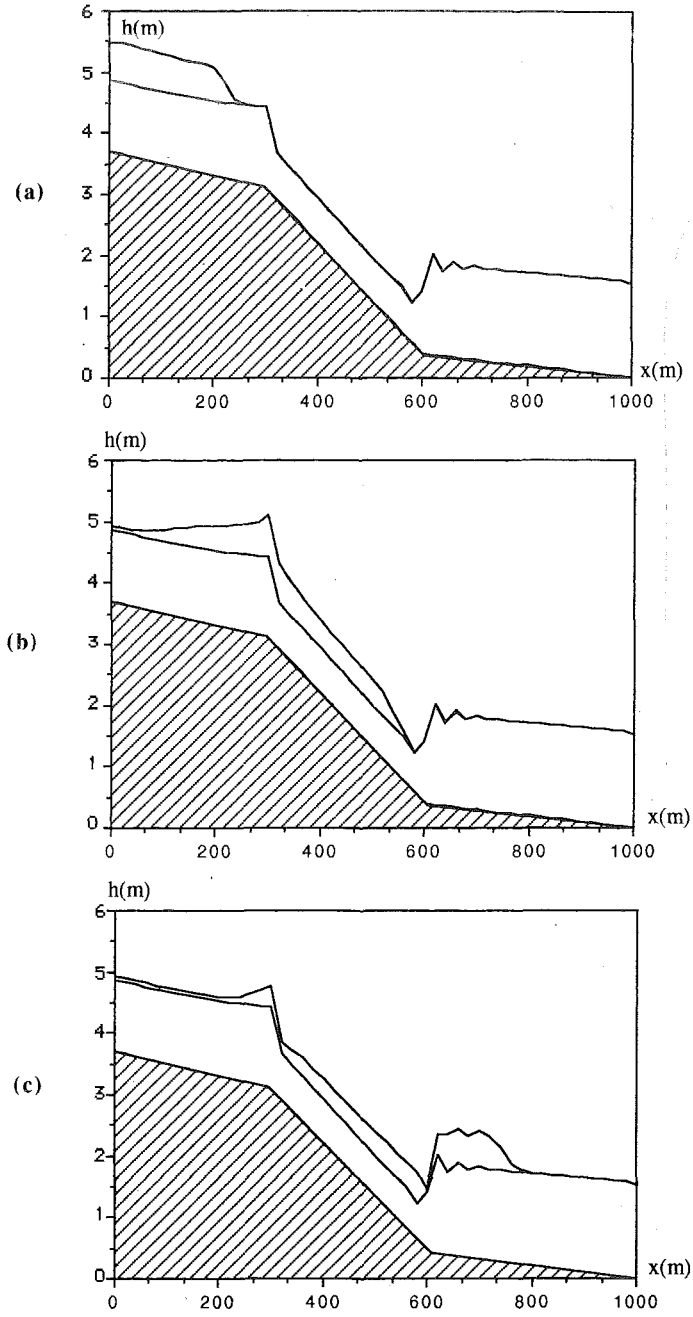

FIG. 2. Flood over Discontinous Steady Profile on Trapezoidal Channel: (*a*) Initial Development of Flood (t = 29 s); (*b*) At t = 70 s; (c) At t = 109.5 s

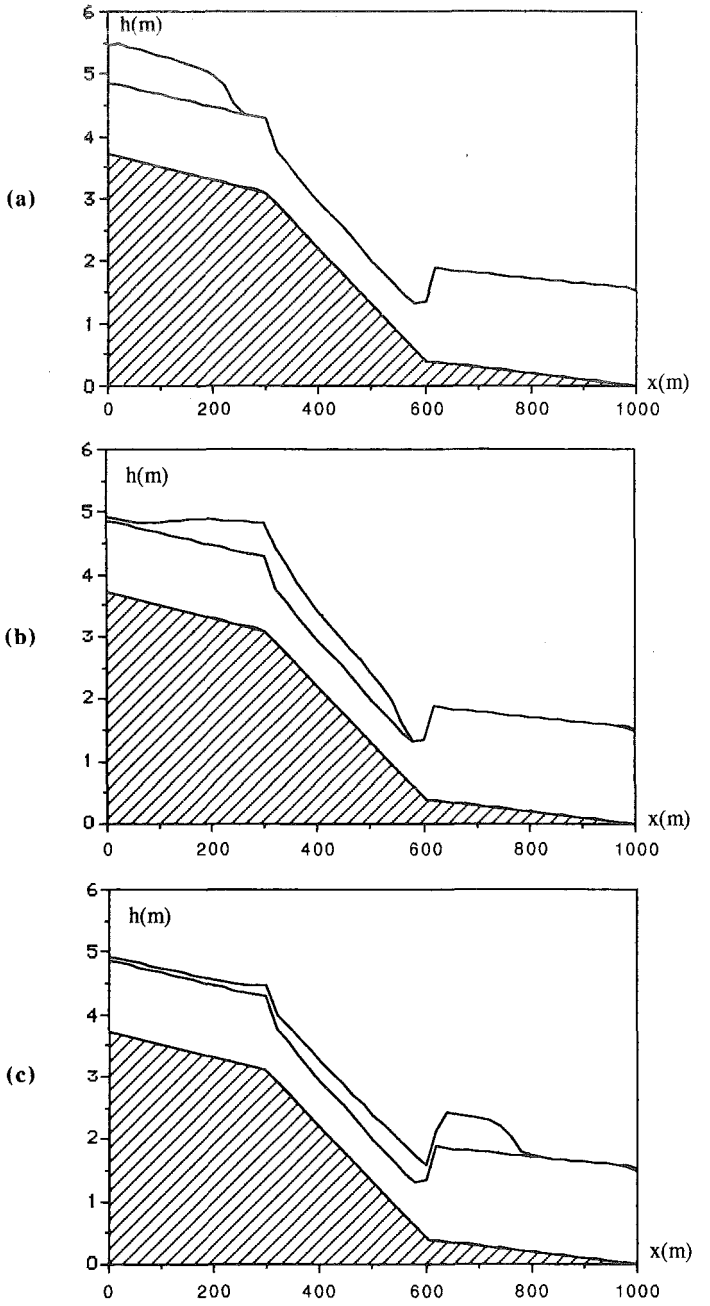

FIG. 3. Flood over Discontinuous Steady Profile on Trapezoidal Channel: (*a*) Initial Development of Flood (t = 29 s); (*b*) At t = 70 s; (*c*) At t = 109.5 s

with $H_v = 0.25$ m. The unsteady situation at three different times ($t_a = 29$ s; $t_b = 70$ s; and $t_c = 109.5$ s) can be seen in Fig. 2 as computed with the classical McCormack scheme and in Fig. 3 as computed with the TVD McCormack scheme. Note that the Fig. 2 displays a rather oscillating solution near the hydraulic jump and a strange behavior at the upper bed transition. The abrupt changes in the bottom slope and the extreme flow conditions do not have a serious effect on the numerical solution of Fig. 3, which shows up stable and well behaved everywhere, not only for the steady (initial) state but also for the unsteady situation.

Flow over Bump

Fig. 4 shows the comparison of the numerical results obtained with the modified McCormack scheme and the exact solution for the stationary case of a rectangular channel 1 m wide with variable bottom slope in the shape of a bell-shaped curve. At the upstream end a constant head of 10 m is imposed, while downstream water depth is held fixed at a value of 6 m. These conditions lead to a subcritical accelerating flow before the bump, which reaches critical conditions at its top and then becomes supercritical downhill. A hydraulic jump must develop at some location to connect the supercritical profile with the subcritical one imposed by the downstream boundary condition.

An exact solution can be calculated for each point in the channel by solving a cubic equation that derives from imposing conservation of water head for each branch. The two profiles on each side of the shock are connected by the jump relations.

An initial situation of constant discharge and water stage is marched in time toward the steady state using the McCormack scheme with the additional proposed TVD step [(12)]. As can be seen from Fig. 4, the agreement with the exact solution is very good despite the low number (41) of mesh points used. The numerical results follow closely all regimes of flow with a smooth transition from subcritical to supercritical at the top of the bump, and the shock is sharply captured at the correct location without any over- or undershoot.

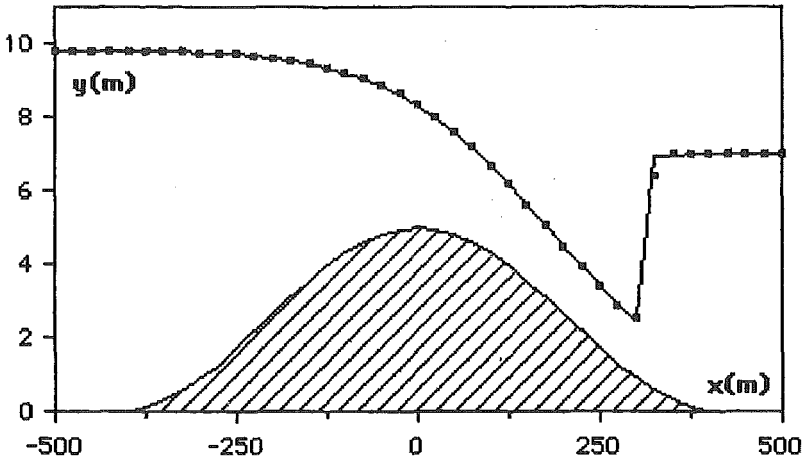

FIG. 4. Steady Frictionless Flow over Bump in Rectangular channel (—— = Analytical Solution; ■ = Numerical Solution)

Steady Flow in Converging-Diverging Channel

Another interesting test case for the analysis of the algorithm performance is that of the flow across a contracted section in a rectangular, horizontal and frictionless channel. The width variation modifies the steady-state profiles as well as those of the propagating fronts. This example is related to many practical problems such as flow between bridge piers or flood-wave propagation along waterways of irregular cross section.

In a 500 m long channel, a sinusoidal width variation is supposed to exist between $x = 100$ m and $x = 400$ m from a maximum value of $b = 5$ m. The first example is the determination of the equilibrium profile of the water for a discharge of $Q = 20$ m^3/s. Subcritical initial conditions are stated at a depth $y(x, 0) = 2$ m and a 0.01 m high weir condition is imposed at the downstream boundary. As Fig. 5 makes plain, the water accelerates as it approaches the point of maximum contraction. Having chosen this parameter as the critical contraction width ($b_c = 3.587$ m in our example), the flow becomes critical there. It changes then to supercritical flow, which gives rise to a stationary hydraulic jump to connect with the subcritical profile required by the downstream condition.

The numerical solutions obtained with the McCormack scheme are displayed with [Fig. 5(a,] and without [Fig. 5(b)] the third step [(12)]. The exact solution is calculated for this situation following a method akin to that of the previous example and is plotted for comparison. It may be verified that the presence of the limiter makes the numerical solution follow closely the exact solution, avoiding oscillations. The agreement seems to be quite good. The CFL number is 0.95 for Fig. 5(a) and 1 for Fig. 5(b), with 51 mesh points having been used.

Surge Propagation through Converging-Diverging Channel

Finally, the time evolution of a surge in a channel of the previous shape is considered. A bore 9.79 m deep of 1,000 m^3/s (Froude number of 2.09) propagates downstream over still water 1 m deep. The comparison between the results given by the two versions of the McCormack scheme are displayed in Fig. 6. The situation at $t = 5$ s can be seen in Fig. 6(a). A 2 m weir is supposed to be placed downstream hence initially closing the channel end.

As the supercritical front advances through the contracting channel it increases its height and decelerates. Once the point of maximum contraction (here chosen not to be the critical one) is surpassed, the front starts lowering and accelerating again. Fig. 6(b) displays the system at $t = 15$ s. In Fig.

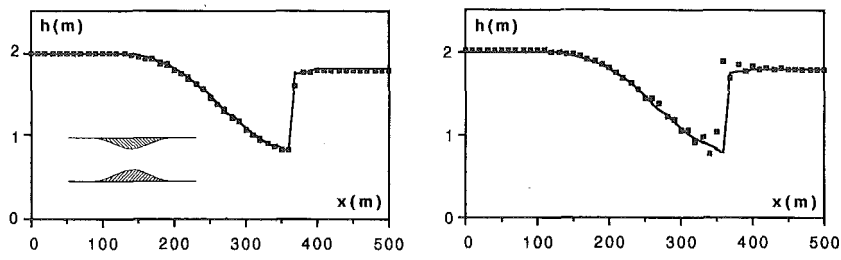

FIG. 5. Stationary Flow in Channel of Variable Width (—— = Analytical Solution; ■ = Numerical Solution): (*a*) Computed with McCormack TVD scheme; (*b*) Computed with McCormack Classical Scheme

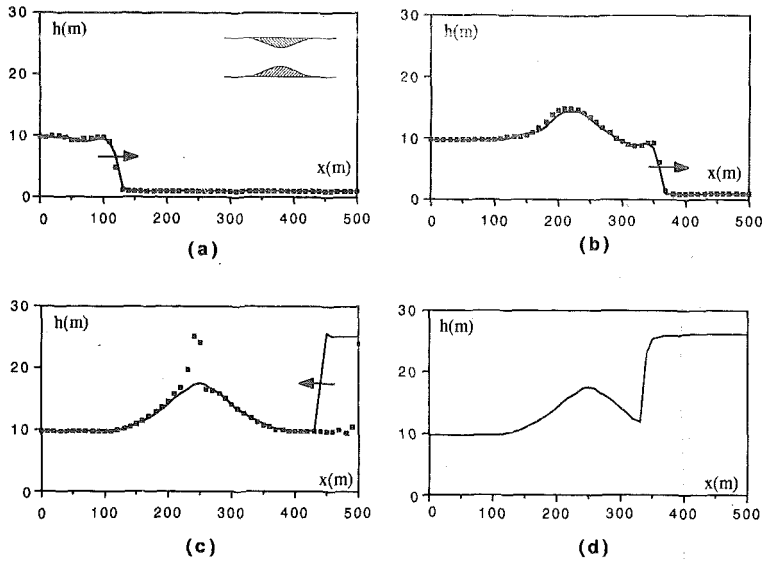

FIG. 6. Sequences of Unsteady Flow Resulting When Bore Propagates over Still Water into Channel of Variable Cross Section at: (*a*) t = 5 s; (*b*) t = 15 s; (*c*) t = 150 s; (*d*) Stationary Solution Reached at t = 600 s (—— = Computed with McCormack TVD Scheme; ■ = Computed with McCormack Scheme)

6(a, b), a rather similar performance of the two methods can be observed. The downstream end is then reached by a front similar to the initial one so that it is partially reflected and partially transmitted over the weir. The slow reflected surge 25.25 m deep starts traveling upstream as can be seen in Fig. 6(c) (t = 150 s). It is worth noting here that the height of the reflected front simultaneously satisfies the jump equations together with the weir condition. The front propagates until it becomes a stationary hydraulic jump at a certain location in the contracting region.

The final steady state is shown in Fig. 6(d) (t = 600 s). Note that due to the usual production of spurious oscillations around discontinuities, the computation with the scheme of McCormack without limiter introduces a new hardship: The scheme was not able to accurately represent the reflected front and, consequently, it furnished a wrong front celerity, which prevented it from advancing upstream, thus vitiating the solution. The reason why no comparison is shown in Fig. 6(d) is that the calculation using the classical McCormack scheme failed after t = 150 s. From a technical point of view it is important to remark that serious mistakes can be introduced by the limitations of a given numerical scheme, as this example makes plain.

CONCLUSIONS

The addition of a conservative dissipation step to the widely used McCormack numerical scheme for solving the one-dimensional open-channel-flow equations was implemented. The extra step was devised according to the theory of total variation diminishing (TVD) schemes.

The algorithm is capable of capturing sharp discontinuities without generating spurious oscillations.

The modification does not introduce any additional difficulty in the treatment of the source terms of the equations, and it is easily introduced into existing McCormack based codes.

The time-step limitation for stability remains approximately the same as for the original scheme.

Results from several computations show that the overall performance of the method can be considered as very good and allows for accurate open-channel flow computations involving hydraulic jumps and bores.

APPENDIX I. REFERENCES

Cunge, J. A., Holly, F. M., and Verwey, A. (1980). *Practical aspects of computational river hydraulics*. Pitman, London, England.

French, R. H. (1985). *Open-channel hydraulics*. McGraw-Hill, Book Co., Inc., New York, N.Y.

García-Navarro, P. (1989). "Estudio de la propagación de ondas en cursos fluviales" (in Spanish), PhD thesis, University of Zaragoza, Zaragoza, Spain.

García-Navarro, P., and Savirón, J. M. (1992). "McCormack's method for the numerical simulation of one-dimensional discontinuous unsteady open channel flow." *J. Hydr. Res.*, 30(1), 95–105.

Glaister, P. (1988). "Approximate Riemann solutions of the shallow water equations." *J. Hydr. Res.*, 26(3), 293–306.

Gunaratnum, D. J., Perkins, F. E. (1970). "Numerical solution of unsteady flows in open channels." *Report No. 127*, Massachusetts Institute of Technology, Cambridge, Mass.

Harten, A., and Hyman, P. (1983). "Self adjusting grid methods for one-dimensional hyperbolic conservation laws." *J. Computational Physics*, (50), 235–269.

Harten. A. (1984). "On a class of high resolution total-variation-stable finite difference schemes." *SIAM J. Numerical Analysis*, 21(1), 1–23.

Hirsch, C. (1990). *Numerical computation of internal and external flows. Vol. 2: Computational methods for inviscid and viscous flows*, John Wiley and Sons, Chichester, England.

Huang, J., and Song, C. C. S. (1985). "Stability of dynamic flood routing schemes." *J. Hydr. Engrg.*, ASCE, 111(12), 1497–1505.

Lax, P., and Wendroff, B. (1960). "Systems of conservation laws." *Comm. Pure and Appl. Mathematics*, Vol. XIII, 217–237.

McCormack, R. W. (1971). "Numerical solution of the interaction of a shock wave with a laminar boundary layer." *Proc. 2nd Int. Conf. on Numerical Methods in Fluid Dynamics*, M. Holt, ed., Springer-Verlag, Berlin, Germany, 151–163.

Roe, P. L. (1981). "Approximate Riemann solvers, parameter vectors and difference schemes." *J. Computational Physics*, (43), 357–372.

Roe. P. L. (1984). "Efficient construction and utilisation of approximate Riemann solutions." *Computing methods in applied sciences and engineering*, R. Glowinski, ed., North Holland, Amsterdam, The Netherlands, 499–518.

Roe, P. L. (1989). "A survey on upwind differencing techniques." *Lecture Series in CFD*, Von Karman Institute for Fluid Dynamics, Brussels, Belgium.

Stoker, J. J. (1957). *Water waves*. Wiley Interscience, New York, N.Y.

Sweby, P. K. (1982). "A modification of Roe's scheme for entropy satisfying solutions of scalar non-linear conservation laws." *Numerical Analysis Report*, University of Reading, England.

Sweby, P. K. (1984). "High resolution schemes using flux limiters for hyperbolic conservation laws." *SIAM J. Numerical Analysis*, 21(5), 995–1011.

Yee, H. C. (1989). "A class of high-resolution explicit and implicit shock-capturing methods." *NASA-TM 101088*, National Aeronautics and Space Administration (NASA), Washington, D.C.

Appendix II. Notation

The following symbols are used in this paper:

A = surface area of channel cross section;
a = characteristic speed;
$\tilde{a}$ = approximate characteristic speed;
b = rectangular channel width;
CFL = Courant-Friedrichs-Levy number;
c = speed of propagation of small perturbations (speed of sound);
$\tilde{c}$ = approximate speed of sound;
D = artificial viscosity term;
$\mathbf{e}$ = eigenvector of Jacobian matrix of flux;
$\tilde{\mathbf{e}}$ = eigenvector of approximate Jacobian associated with $\tilde{a}$;
$\mathbf{F}$ = flux vector function;
$\mathbf{G}$ = vector containing source terms;
$\mathbf{g}$ = acceleration of gravity;
H_v = weir height;
h = water depth;
I_1 = hydrostatic pressure force term;
I_2 = force due to channel width variations;
$\mathbf{J}$ = Jacobian matrix of flux;
n = Manning rugosity coefficient;
Q = flow rate;
r = ratio of wave intensities for two consecutive mesh points on which limiting functions depend;
S_0 = bottom slope;
S_f = friction slope;
t = time;
$\mathbf{U}$ = vector containing dependent variables;
u = water velocity;
$\tilde{u}$ = approximate water velocity for two consecutive mesh points;
x = space coordinate;
α = wave intensities for two consecutive mesh points;
Δt = time increment;
Δx = mesh spacing;
δ = small dimensionless number;
λ = ratio $\Delta t/\Delta x$;
σ = general cross-section width at free surface;
φ = limiting function; and
Ψ = entropy correction function.

Superscripts

n = time level.

Subscripts

j = mesh point; and
max = maximum value attainable by a function or variable.

J. Hydraul. Eng. 1992.118:1359-1372.